Chapter One

Introduction

1.1 Zinc Oxide

Recently, zinc oxide (ZnO) has attracted much attention within the scientific community as a ‘future material’. This is however, somewhat of a misnomer, as ZnO has been widely studied since 1935 [1], with much of our current industry and day-to-day lives critically reliant upon this compound. The renewed interest in this material has arisen out of the development of growth technologies for the fabrication of high quality single crystals and epitaxial layers, allowing for the realization of ZnO-based electronic and optoelectronic devices.

ZnO crystallises in three forms: zincblende, wurtzite, and rocksalt crystals [2]. The two common crystal structures of ZnO are the wurtzite and zincblende structures, whereas the rocksalt structure can be formed at high pressures at about 10 GPa [3].

1.2 objectives

The main objective of this project was to explore the effect of substitution of Zinc atoms by Strontium atoms in Zinc oxide compound. The Structure and electronic behaviors of Strontium Zinc Oxide have been studied as predict that this new compound will have many optical applications.

1.3 Literature review

Wurtzite ZnO can be represented by a hexagonal unit cell with two lattice parameters a and c as shown in Figure 1.1. Within the unit cell, the structure comprises two interpenetrating hexagonal closed-packed (hcp) sublattices, each

of which contains four atoms in a unit cell. Here, each atom of one kind is surrounded by four atoms of the other kind (i.e. tetrahedral coordination), in other words, each sublattice consists of one type of atom displaced from the other along the threefold c-axis by an amount u = b/c (the internal parameter u is defined as the length of the bond parallel to the c-axis divided by the c lattice parameter). The u parameter has been defined as 0.375 for an ideal wurtzite structure [4]. However, as real wurtzite ZnO crystals tend to deviate from the ideal conformation, the u parameter

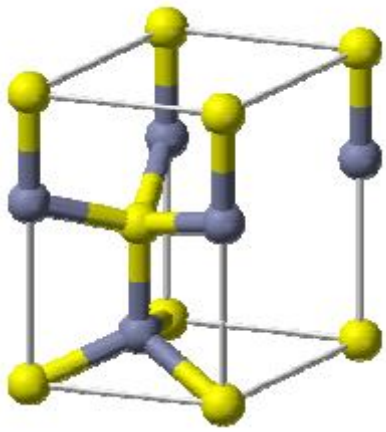

Figure (1.1): Unit cell of wurtzite ZnO[4]

may deviate from the ideal value, giving an increased value when the c/a ratio decreases.

The lattice parameters for wurtzite ZnO are commonly measured via x-ray diffraction (XRD) based methods experimentally and using first principles calculations theoretically . The lattice parameters (a, b and c) of the wurtzite ZnO

with an internal parameter (u), that have been reported previously and obtained experimentally and theoretically, show that the a and c values range from 3.166 to 3.298 Å, and from 5.070 to 5.294 Å, respectively . The c/a ratio and the u parameter range from 1.572 to 1.617, and from 0.376 to 0.389, respectively.

3d-transition-metal-doped ZnO film ~n-type Zn12MxO (x50.05): M5Co, Mn, Cr, Ni! Are formed on sapphire substrates using a pulsed-laser deposition technique, and their magnetic and electric properties are examined. The Co-doped ZnO films showed the maximum solubility limit.

Some of the Co-doped ZnO films exhibit ferromagnetic behaviors with the Curie temperature higher than room temperature. The magnetic properties of Co-doped ZnO films depend on the concentration of Co ions and carriers [5].

1.4 Problem

The problem of this project long time was to explore the effect of substitution of Zinc atoms by Strontium atoms in Zinc oxide compound. The Structure and electronic behaviors of Strontium Zinc Oxide have been studied as predict that this new compound will have many optical applications.

1.5 Outline of the thesis

Thesis content four chapters:

The chapter one introduction, the chapter two Density Functional Theory (DFT),

The chapter three Defect in Solid, the four Results and Discussion.

Chapter two

Density functional theory (DFT)

2.1 Introduction

The motivation of density functional theory (DFT) is to avoid trying to solve the many electron wave function $\Psi(r_1, r_2, r_i, \ldots . r_n)$ as in the Hartree-Fock method, by instead solving for the electron density distribution $\rho(r)$.

Density functional theory is based on the 1964 theorem of Hohenberg and Kohn [6] and the computational scheme by Kohn and Sham [7]. It is based on the idea that every ground state observable property of a quantum mechanical system can be calculated from the charge density, and that a given ground state electron density cannot arise from two different external potentials, unless the two differ by a constant, i.e. the ground state electronic structure is uniquely determined by the electron density.

2.2 Hohenberg-Kohn theorem

Hohenberg and Kohn [8, 9, 10] formulated two basic theorems of the DFT:

The first theorem states that the ground-state density $\rho(r)$ of a bound system of interacting electrons in an external potential υ (r) determines this potential uniquely. In other words there exist a one-to-one correspondence between the electron density of a systems and the energy and hence all properties of the system can be considered to be unique functionals of ground state density. They consider a potential $\upsilon_1(r)$ that gives an electron density $\rho(r)$. Now assume

another potential $v_2(r)$ that gives the same density. These potentials would give two Hamiltonians

that have the same H_1andH_2 ground state density where,

$$H_1 = \mathrm{T} + U + \sum_i v_1(r_i) \quad ; \quad H_2 = \mathrm{T} + U + \sum_i v_2(r_i) \tag{2.1}$$

Where

$$\mathrm{T} = -\frac{1}{2}\sum_i^N \nabla_i^2 \quad \text{and} \quad U = \frac{1}{2}\sum_{i\neq j}\frac{1}{|r_i - r_j|}$$

with the corresponding Schrödinger equation, $H_1\Psi_1 = E_1\Psi_1$and $H_2\Psi_2 = E_2\Psi_2$, and we assume that the two wave function $\Psi_1$and Ψ_2 yield that same density as,

$$\rho(r_i) = N\int \Psi^*(r_1, r_2, .., r_N)\Psi(r_1, r_2, .., r_N)dr_2 dr_3 .. dr_N \tag{2.2}$$

Now, by variational method,

$E_1 = \langle\Psi_1|H_1|\Psi_1\rangle$

$< \langle\Psi_2|H_1|\Psi_2\rangle$

$< \langle\Psi_2|H_2|\Psi_2\rangle + \langle\Psi_2|H_1 - H_2|\Psi_2\rangle$

$$E_1 \leq E_2 + \int \rho(r)[v_1(r) - v_2(r)]\, dr \tag{2.3}$$

Similarly,

$E_2 = \langle\Psi_2|H_2|\Psi_2\rangle$

$< \langle\Psi_1|H_2|\Psi_1\rangle$

$< \langle\Psi_1|H_1|\Psi_1\rangle + \langle\Psi_1|H_2 - H_1|\Psi_1\rangle$

$$E_2 \leq E_1 - \int \rho(r)[v_1(r) - v_2(r)]dr \quad (2.4)$$

Adding the above two inequalities (2.3) and (2.4) gives the contradiction

$$E_1 + E_2 < E_2 + E_1 \quad (2.5)$$

Therefore, it can be deduced that there cannot be two different potentials that yield the same ground state electron density. Moreover, the external potential $v(r)$is a unique functional of density$\rho(r)$. This shows that it is possible to rewrite the Schrödinger equation in term of the density.

2.3 Periodic Supercell and K- point sampling

In a periodic crystal, the fundamental unit cell is repeated to form an infinite system. Even though the periodicity can be in one, two or three dimensions, the later one is far more common and is characterized by three vectors , a_1, a_2, and a_3 spanning a vector space. Any single point in this direct lattice space is characterized by a vector r(i.e., a linear combination of a_1, a_2, and a_3**)**. In the same manner there exists a unique reciprocal space, corresponding to each direct cell, defined by the reciprocal vectors ,b_1, b_2, and $b_3$derived from a_1, a_2, and a_3 obeying the orthonormality relation $a_i b_j = 2\pi\delta_{ij}$. In reciprocal space the fundamental building block is called the first Brillouin zone. As in the case of direct lattice space, each point in the reciprocal space is uniquely represented by a vector k (usually designated as the wave vector). Since the lattice is periodic in nature, the potential energy of the crystal must also be periodic in nature, such that for a translation by any direct lattice vector g the potential energy does not change,

$$V(r-g) = V(r) \tag{2.6}$$

Because of the symmetry constraints, the Schrödinger equation given in equation (2.1) should also be translation invariant; indicating that for a translation of the whole crystal by a lattice vector *g*, the solution of the equation,

$$H(r+g)\psi(r+g) = E\psi(r+g) \tag{2.7}$$

agree with those of equation (2.1). According to Bloch theorem [11,12], the eigenfunctions with the correct symmetry relative to a potential of the form in equation. (2.7) has the form of a plane wave times function with the periodicity of the lattice,

$$\Phi(r+k;g) = \exp[ik.g]\,\Phi(r;k) \tag{2.8}$$

Here $\Phi(r;k)$ is called the Bloch function(BF) and they span an infinite crystal. The wave vector *k* labels the different solutions to the Schrödinger equation given in equation (2.1). The BF has the following form,

$$\Phi(r;k) = \exp[ik.r]\,u(r,k) \tag{2.9}$$

Here *u*(*r*, *k*) has the same periodicity of the lattice. Alternatively, Bloch theorem indicates that a crystalline orbital (CO), $\psi_{n,k}(r)$corresponding to the n^{th} band in the unit cell can be written as a wave like part and a cell periodic part $\varphi_n(r)$ called the "Bloch orbital":

$$\psi_{n,k}(r) = \exp[ik.r]\,\varphi_n(r). \tag{2.10}$$

The beauty of BFs is that they have interesting translational properties in reciprocal space. Consider a point k 'in the reciprocal lattice obtained by the translation of k by any reciprocal lattice vector K. If we apply Bloch theorem to the corresponding BF,$\Phi(r;k')$, it is evident that $\Phi(r;k')$ exhibits the same translational properties

as $\Phi(\mathrm{r}, \mathrm{k})$,

$$\Phi(r + g; k') = \exp[i(k + K).g\Phi(r; k + K)$$

$$= \exp[ik.g]\,\Phi(r; k') \qquad (2.11)$$

and one would immediately see not only that $\Phi(r; k')$ and $\Phi(\mathrm{r}, \mathrm{k})$ can be referred to the same k, but also that both of them are acceptable eigenfunctions of that k in equation (2.1). This behavior of BF allows us to restrict our analysis only to the first Brillouin zone. In fact the use of BFs has to be associated with the integration over the first Brillouin zone and would require *a priori* compute different quantities at a large number of k-points. In principle, the electronic wave functions at k points which are close to each other are almost identical, hence they are solved at a finite set of k points and the results can be interpolated.

Several methods for k point sampling have been proposed in the literature. In our calculations we use the scheme proposed by Monkhorst and Pack [13] for calculating the electronic states at a set of k points in the Brillouin zone. Other methods for the k points sampling were developed by Chadi and Cohen [14], and Joannopoulos and Cohen [15]. Using these methods one can obtain an accurate approximation for the electronic potential and the total energy of an insulator or a semi-conductor by calculating the electronic states at a very small number of k points.

2.4 The CRYSTAL06 Code

The CRYSTAL package performs ab initio calculations of the ground state energy, electronic wave function and properties of periodic systems. Hartree-

Fock and Kohn-Sham Hamiltonians can be used. Systems that are periodic in zero

(molecules, 0D), one (polymers, ID), two (slabs, 2D) and three dimensions (crystals, 3D) can be treated [58]. In each case, the fundamental approximation made is the expansion of the single particle wave functions $\psi_i(r; k)$ ("Crystalline orbital", CO) as a linear combination of Bloch functions (BF), defined in terms of local functions (hereafter called as "Atomic orbitals", AOs) [16,17]. The AOs are contracted linear spherical harmonic Gaussian Type Functions (GTFs), optimized for the crystalline environments. Analytically the *GTF* χ_α^{GTF}has the following form,

$$X_\alpha^{GTF} = \exp(-\alpha r^2)\, x^l y^m z^n \qquad (2.12)$$

where α is the exponent and the *l, m,* and *n* are simply powers of the Cartesian coordinates. With the increase in the size of the basis set, the CPU time and the amount of disk space needed to store the temporary integrals increases dramatically. Thus one has to expand the orbital with less number of basis set without losing the accuracy. In most applications this is achieved by expanding the Gaussian functions as a contraction of individually normalized Gaussian primitives $g_j(r)$. They are characterized by the same center and angular quantum numbers but with different exponents:

$$x_i(r) = \sum_{j=1}^{s} d_j g_j(r) \qquad (2.13)$$

where

$$g_j(r) = g(r^{\cdot}, \alpha, l, m) = N_{lm}(\alpha) r^l Y_{lm}(\theta, \phi) \exp\left(-\alpha_j r^2\right) \qquad (2.14)$$

where s is the length of the contraction, α_j is a contraction exponent, d_j is a contraction coefficient. The Gaussian primitives are written in terms of real spherical harmonics including normalization constant. The exponents and the

contraction coefficients are normally chosen on the basis of relative cheap atomic SCF calculations so as to give basis functions suitable for describing the exact Hartree-Fock atomic orbitals (CRYSTAL06 code).

By proper choice of these quantities, the resulting contracted Gaussians can be used to mimic any functional form. Therefore one has to choose the exponents and the contraction coefficients of the primitives so as to lead the basis functions towards the desired properties. A typical basis set will have certain core functions with a large number of primitives and relatively large exponents. On the other hand the valence functions will have only few primitives with lower exponents. Basically, the core states are not in general affected by changes in chemical bonding. Hence, in order to reduce the computational expenses, especially for heavier atoms, the core states can be replaced by Pseudopotentials. The idea behind the Pseudopotentials is to treat the core electrons by their effect on the potential filled by the electrons in the valence shell by slightly modifying the Hamiltonians and moreover it is easier to incorporate relativistic effects in Pseudopotentials formalism. High quality Gaussian basis sets are adopted for the present study. For heavier atom like strontium, Pseudopotentials are used to treat the core electrons.

2.5 Implementation of hybrid functionals

In a series of papers [18,19] Becke examined the effects of exchange and correlation in DFT on the computation of thermo chemical properties. In examining the role of exact exchange, he demonstrated the inclusion of a small component of exact-exchange within the DFT exchange-correlation approximation lead to more accurate molecular energetic.

The exchange-correlation approximation proposed by Becke was:

$$E_{xc} = (1 - A)E_{xc}^{LDA} + AE_{x}^{EXACT} + B\Delta E_{x}^{B88} + E_{c}^{LDA} + C\Delta E_{c}^{PW91} \qquad (2.15)$$

where exact E_x^{EXACT} is the exact exchange energy, $\Delta E_x^{B88}$is Becke's gradient correction to the exchange functional, and $E_c^{PW91}$is the Perdew and Wang gradient corrected correlation. The parameters *A*, *B*, and *C* are semi-empirical coefficients that were determined by a least-squares fit to atomization energies, ionization potentials, and electron and proton affinities in Pople's test set [20,21] of atomic and molecular species, and Becke suggested values of *A* = 0.2, *B* = 0.72, and *C* =

0.81.

When this method was implemented in the Gaussian 92 code, the Perdew and Wang correlation was replaced by the Lee-Yang-Parr [22] (LYP) correlation and this hybrid functional was called B3LYP. As the LYP functional does not have an easily separable local component, it was proposed the use of the exact form of Vosko-Wilk-Nusair (VWN) [23] correlation potential corresponding to a fit to the Ceperley-Alder Monte Carlo simulation data is used for the correlation correction and The B3LYP functional takes the following explicit form:

$$E_{xc}^{B3LYP} = (1 - A)E_x^{LDA} + AE_x^{HF} + B\Delta E_x^{B88} + CE_c^{LYP} + (1 - C)E_c^{VWN} \quad (2.16)$$

This functional is the implementation of B3LYP within the CRYSTAL package, and consequently the implementation used in this thesis.

Chapter three

Defect in solid

3.1 Introduction

It is useful to classify crystal lattice defects by their dimension. The 0-dimensional defects affect isolated sites in the crystal structure, and are hence called point defects. an example is a solute or impurity atom, which alters the crystal pattern at a single point. The 1-dimensional defects are called dislocations. They are lines along which the crystal pattern is broken. The 2-dimensional defects are surfaces, such as the external surface and the grain boundaries along which distinct crystallites are joined together. The 3-dimensional defects change the crystal pattern over a finite volume.

They include precipitates, which are small volumes of different crystal structure, and also include large voids or inclusions of second-phase particles.

Any deviation from the perfect atomic arrangement in a crystal is said to contain imperfections or defects. In fact, using the term “defect” is sort of a misnomer since these features are commonly intentionally used to manipulate the mechanical properties of a material. Adding alloying elements to a metal is one way of introducing a crystal defect. Crystal imperfections have strong influence upon many properties of crystals, such as strength, electrical conductivity and hysteresis loss of ferromagnetism. Thus some important properties of crystals are controlled by as much as by imperfections and by the nature of the host crystals.

1- The conductivity of some semiconductors is due entirely to trace amount of chemical impurities.
2- Color, luminescence of many crystals arise from impurities and imperfections.

3- Atomic diffusion may be accelerated enormously by impurities or imperfections

Mechanical and plastic properties are usually controlled by imperfections[24].

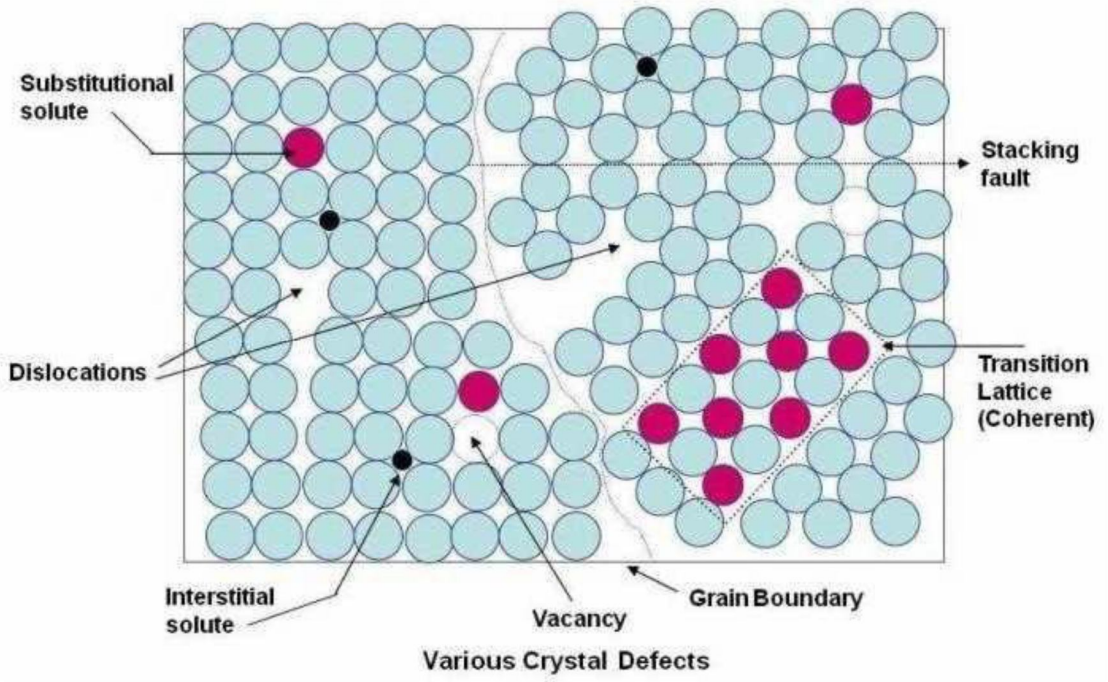

Figure(3.1) shows defect in solid[24].

3.2 Point defects

A point defect disturbs the crystal pattern at an isolated site. It is useful to distinguish intrinsic defects, which can appear in a pure material, from extrinsic defects, which are caused by solute or impurity atoms.

Point defects are defects that occur only at or around a single lattice point. They are not extended in space in any dimension. Strict limits for how small a point defect is are generally not defined explicitly, typically, however, these defects involve at most a few extra or missing atoms. Larger defects in an ordered structure are usually considered dislocation loops. For historical reasons, many point defects, especially in ionic crystals, are called centers: for example a vacancy in many ionic solids is called a luminescence center, a color center, or

F-center. These dislocations permit ionic transport through crystals leading to electrochemical reactions. These are frequently specified using Kröger–Vink Notation.

3.2.1 Vacancy defects

are lattice sites which would be occupied in a perfect crystal, but are vacant. If a neighboring atom moves to occupy the vacant site, the vacancy moves in the opposite direction to the site which used to be occupied by the moving atom. The stability of the surrounding crystal structure guarantees that the neighboring atoms will not simply collapse around the vacancy. In some materials, neighboring atoms actually move away from a vacancy, because they experience attraction from atoms in the surroundings. A vacancy (or pair of vacancies in an ionic solid) is sometimes called a Schottky defect.

3.2.2 Interstitial defects

are atoms that occupy a site in the crystal structure at which there is usually not an atom. They are generally high energy configurations. Small atoms in some crystals can occupy interstices without high energy, such as hydrogen in palladium.

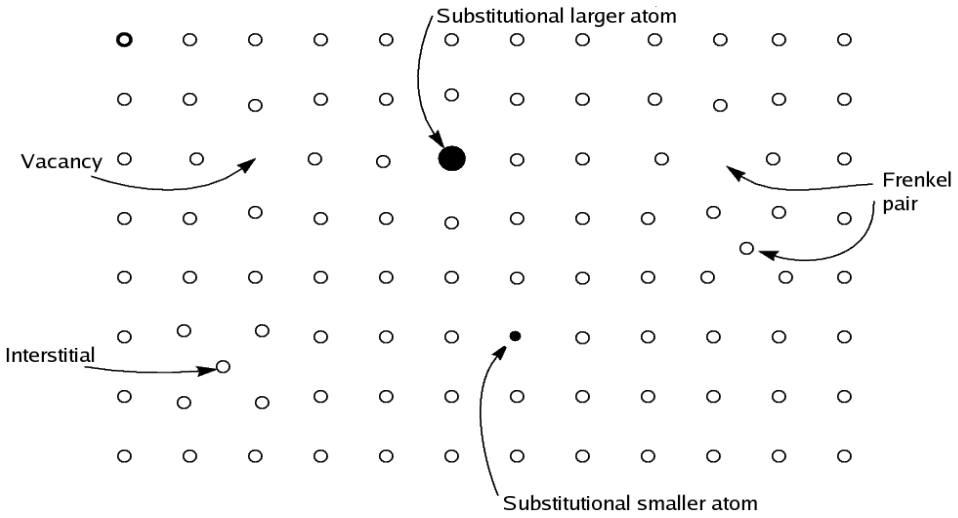

Figure(3.2) Schematic illustration of some simple point defect types in a monatomic solid [25].

3.2.3 Frenkel defect

A nearby pair of a vacancy and an interstitial is often called a Frenkel defect or Frenkel pair. This is caused when an ion moves into an interstitial site and creates a vacancy.

3.2.4 Impurity

Due to fundamental limitations of material purification methods, materials are never 100% pure, which by definition induces defects in crystal structure. In the case of an impurity, the atom is often incorporated at a regular atomic site in the crystal structure. This is neither a vacant site nor is the atom on an interstitial site and it is called a substitutional defect. The atom is not supposed to be anywhere in the crystal, and is thus an impurity. In some cases where the radius of the substitutional atom (ion) is substantially smaller than that of the atom (ion) it is replacing, its equilibrium position can be shifted away from the lattice site. These types of substitutional defects are often referred to as off-center ions. There are two different types of substitutional defects: Isovalent

substitution and aliovalent substitution. Isovalent substitution is where the ion that is substituting the original ion is of the same oxidation state as the ion it is replacing. Aliovalent substitution is . Aliovalent substitutions change the overall charge within the ionic compound, but the ionic compound must be neutral. Therefore, a charge compensation mechanism is required. Hence either one of the metals is partially or fully oxidized or reduced, or ion vacancies are created[25].

3.4 Defect line:

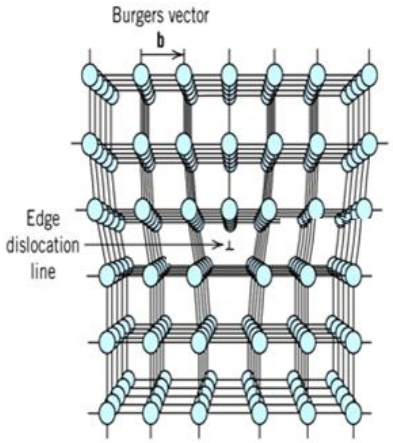

Figure(3.3)show defect line [25].

edge dislocation in a simple cubic structure is drawn in Fig. which shows both a two-dimensional view and a three-dimensional section along the dislocation line. The dislocation can be created by making a cut in the crystal on the dashed plane the left of the dislocation by one lattice spacing, and allowing the atoms to re-bond across the slip plane. This recipe recreates the simple cubic unit cell everywhere except on the dislocation line itself (ignoring the small elastic distortion of the cells that border the dislocation line).

3.5 Defect surfaces

The two-dimensional defects that appear in crystals can be usefully divided into three types: free surfaces, which are the external surfaces at which the solid terminates at a vapor or liquid, inter crystalline boundaries, which separate grains or distinct phases within the solid, and internal defects that disrupt the crystalline pattern over a surface within a crystal. All of these defects have two important characteristics. First, since they are surfaces in a crystal they have particular atomic structures that depend on orientation.

Second, they have a positive energy. The energy per unit area is ordinarily equal to the surface tension.

The interface between a crystalline solid and a vapor or liquid governs the interaction between the two phases, and influences the behavior of the solid in many important ways that we shall discuss later in the course. It also affects the shape of the solid. The shape and properties of the free surface are determined by a combination of its structure and its energy. These two parameters are related to one another.

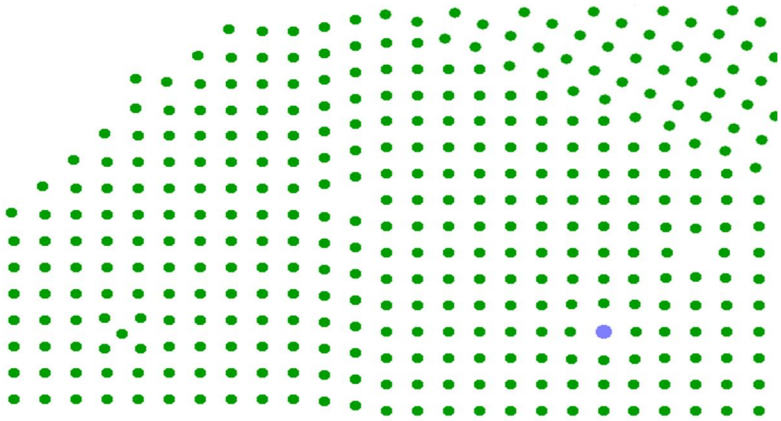

Figure(3.4) :defect in surface [26].

perfect vacuum, the atoms in the free surface are bonded on only one side and the spacing and the configuration of the atoms in the first few planes at the interface adjusts to accommodate the asymmetry of the bonding in the bast possible way. The structure of a real interface is further complicated by bonding

interactions across the interface and by chemical changes in the interfacial plane. The dangling bonds at the interface provide favorable sites for the adsorption of atoms that do not fit well into the bulk lattice. Then interface is often enriched in solute species (surfactants). Oxygen, sulfur and phosphorous are common surfactants in engineering solids[26].

3.6 VOLUME DEFECTS

Volume defects in crystals are three-dimensional aggregates of atoms or vacancies. It is common to divide them into four classes in an imprecise classification that is based on a combination of the size and effect of the particle. The four categories are: precipitates, which are a fraction of a micron in size and decorate the crystal; second phase particles or dispersants, which vary in size from a fraction of a micron to the normal grain size (10-100μm), but are intentionally introduced into the microstructure; inclusions, which vary in size from a few microns to macroscopic dimensions, and are relatively large, undesirable particles that entered the system as dirt or formed by precipitation; and voids, which are holes in the solid formed by trapped gases or by the accumulation of vacancies. Precipitates are small particles that are introduced into the matrix by solid state reactions. While precipitates are used for several purposes, their most common purpose is to increase the strength of structural alloys by acting as obstacles to the motion of dislocations. Their efficiency in doing this depends on their size, their internal properties, and their distribution through the lattice. However, their role in the microstructure is to modify the behavior of the matrix rather than to act as separate phases in their own right. Dispersants are larger particles that behave as a second phase as well as influencing the behavior of the primary phase. They may be large precipitates, grains, or poly granular particles distributed through the microstructure. When a microstructure contains dispersants such properties as mechanical strength and electrical conductivity are some average of the properties of the dispersant phase

and the parent. Inclusions are foreign particles or large precipitate particles. They are usually undesirable constituents in the microstructure[27].

Chapter Four

Results and Discussion

4.1 Introduction

This chapter describes first principles calculations for SrZnO. Study based on DFT method is performed to evaluate structural and electronic properties of Sr doped into ZnO. Because such properties are depends on composition the compound, we performed the calculations with different percentage of Sr dopant.

4.2 Computational Details

The performed a periodic structure calculations of a perfect and doped cubic perovskite $SrMnO_3$ within the framework of density functional theory method [28] using CRYSTAL06 [29] with the hybrid functional B3LYP exchange correlation functionals which consists of the mixture of the non-local exact Hartree-Fock exchange [30] and Generalized Gradient Approximation (GGA) exchange functionals as proposed by Becke's three parameter method combined with the non-local correlation potential of Lee et al. [31]. CRYSTAL06 employs atom-centered Gaussian-type function as basis sets. The basis sets used were all-electron sets on Zn (86-411d31G) [32], O (8-411-d1) [33] and a pseudopotential basis set (HAYWSC-31(3d)) [34] was used for Sr to reduce computational effort.

The XCrysden Software was used for the structural analysis. Moldraw was used for structure visualization. Debian 8.3 Linux were used in all simulations.

4.3 Mothod

The XCrysden Software was used for the structural analysis. Moldraw was used for structure visualization. Debian 8.3 Linux were used in all simulations. The starting point for calculation was to optimize the ZnO geometry. We use supercell 2×2×1 crystal structure of ZnO compound containing 8 zinc atoms and 8oxygen atoms as shown in figure 4.1. The experimentally measured Wurtzite ZnO lattice parameters are a=b=3.249 Å, c=5.204 Å and space group P63mc (186)[35,36] Optimization of lattice parameters was performed. Our calculation gave the optimized lattice constants structure a=3.289 Å, b=3.289 Å, c=5.280Å, which is in agreement with experimental data.

On substitution one Zn by Sr, we found that the band energy decreased to the value 3.28 eV which means improve in the electrical conductivity of the compound. We found also that when the dopant increases the band energy increases too.

A Sr-doped model (Sr:ZnO) was developed from unit cell expansion in the direction of axes a, b and c, resulting at 12.5-100% doping as shown in Table 4.1.

Table 4.1. Description of the unit cells used for simulating the Sr-doping on ZnO.

.

Doped amount(%)	Unit cell expansion	Zn atoms replaced
0	2x2x1	0
12.5	2x2x1	1
25.0	2x2x1	2
37.5	2x2x1	3

50.0	2x2x1	4
62.5	2x2x1	5
75.0	2x2x1	6
87.5	2x2x1	7
100	2x2x1	8

4.4 Results

Band structure is electronic band structure and energy scheme to describe the conductivity of conductor, insulator and semiconductors.

4.4.1 12.5% doping amount of Sr in ZnO

Table 4 .2: $SrZn_7O_8$ optimized cell parameters

parameters	A	B	C	ALPHA	BETA	GAMMA
Before optimized	6.5782	6.5782	5.2803	90	90	120
After optimized	6.7569	6.7569	5.4019	89.9627	90.0372	120.2892

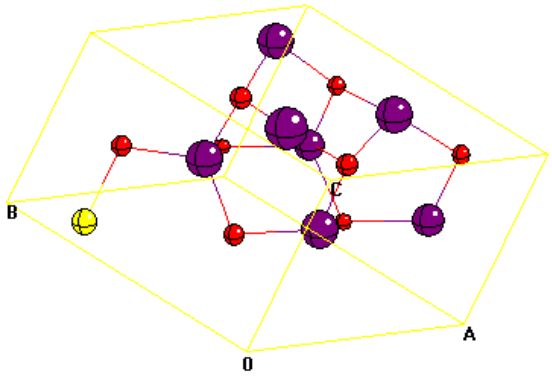

Figure 4.1 $SrZn_7O_8$ crystal structure.

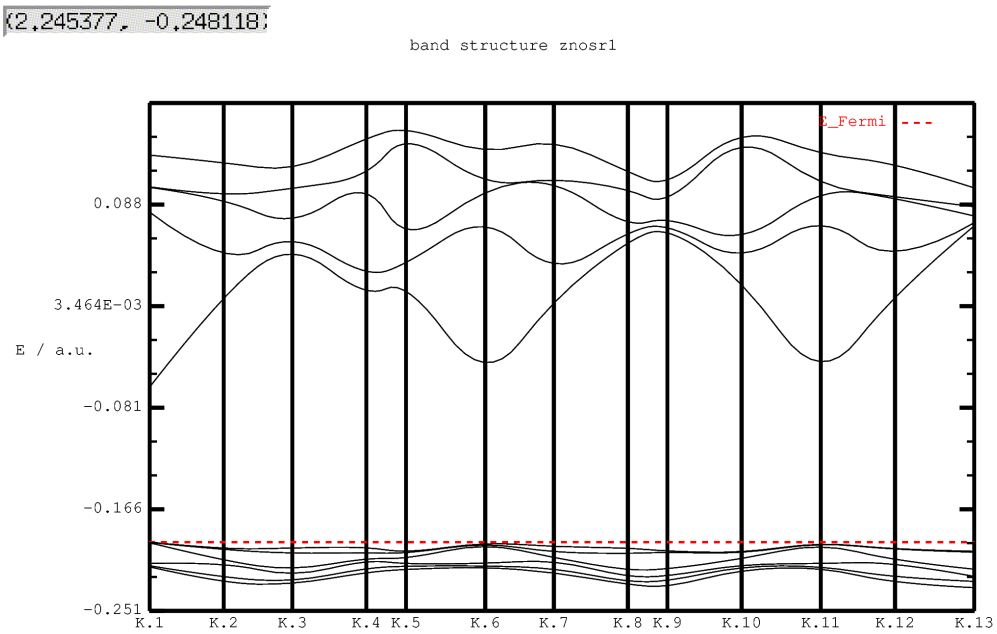

Figure 4.2: Electronic band structure for $SrZn_7O_8$ .The band gap between the top of the valence band and the bottom of the conduction band ≈3.46 electron Volt.

4.4.2 25% doping amount of Sr in ZnO

Table 4 .3: $Sr_2Zn_6O_8$ optimized cell parameters

parameters	A	B	C	ALPHA	BETA	GAMMA
Before optimized	6.5726	6.5726	5.2803	90	90	120
After optimized	6.9258	6.9258	5.5296	90	87.7061	120.0021

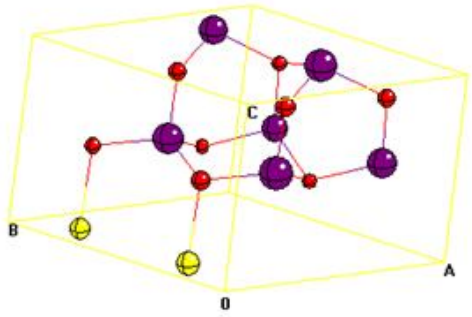

Figure 4.3 $Sr_2Zn_6O_8$ crystal structure.

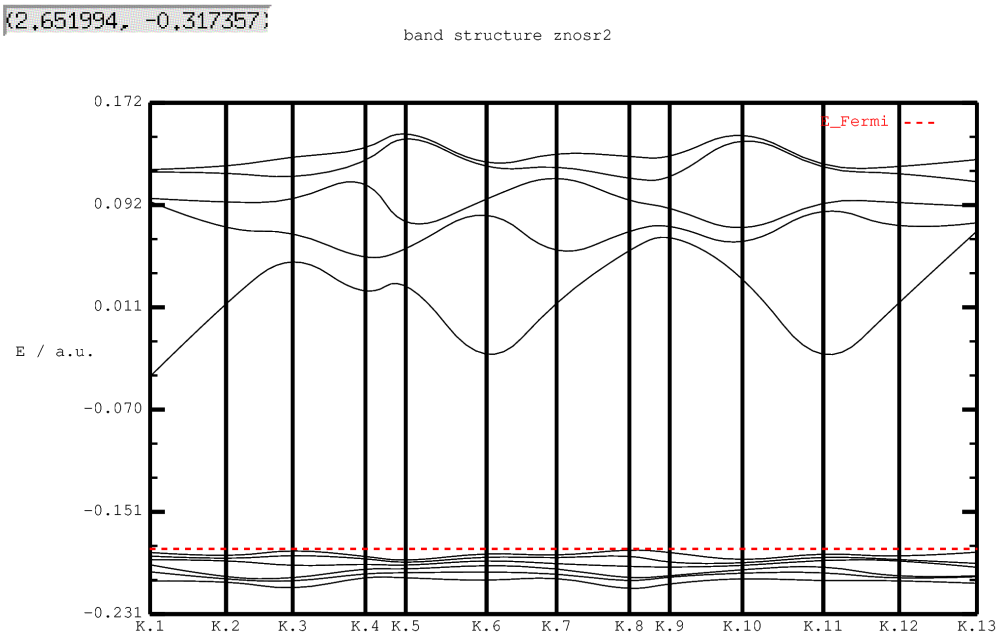

Figure 4.4: Electronic band structure for $Sr_2Zn_6O_8$ .The band gap between the top of the valence band and the bottom of the conduction band ≈3.84 electron Volt

4.4.3 37.5% doping amount of Sr in ZnO

Table 4 .4: $Sr_3Zn_5O_8$ optimized cell parameters

parameters	A	B	C	ALPHA	BETA	GAMMA
Before optimized	6.5782	6.5782	5.2803	90	90	120
After optimized	7.1882	7.1882	5.5630	90	90	120.0021

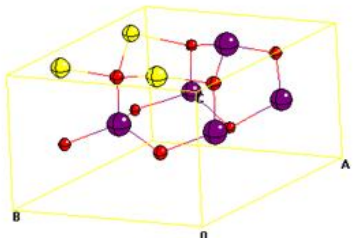

Figure 4.5 $Sr_3Zn_5O_8$ crystal structure.

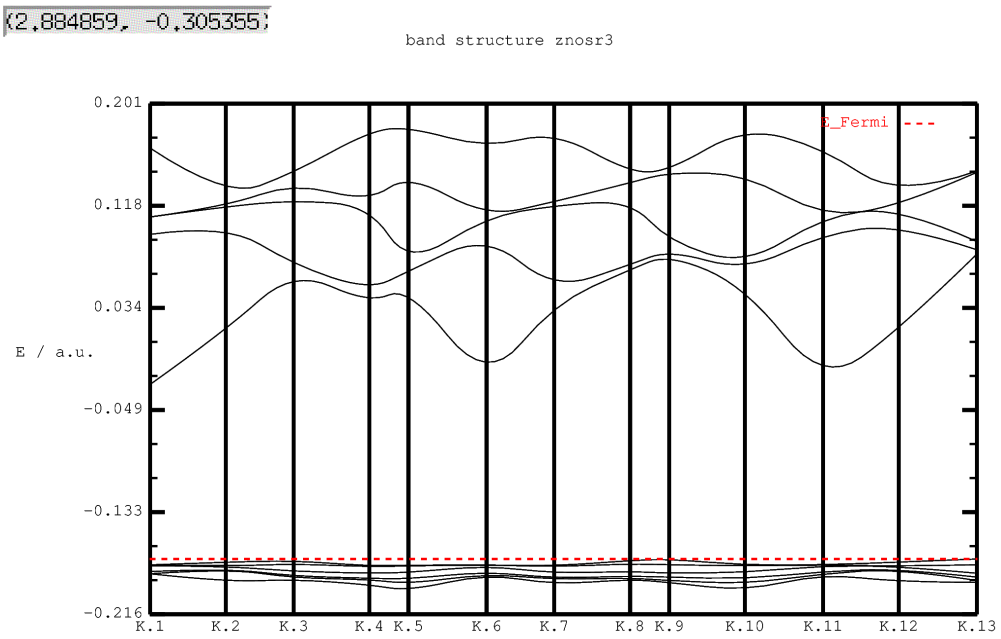

Figure 4.6: Electronic band structure for $Sr_3Zn_5O_8$ .The band gap between the top of the valence band and the bottom of the conduction band ≈3.94 electron Volt.

4.4.4 50% doping amount of Sr in ZnO

Table 4 .5: $Sr_4Zn_4O_8$ optimized cell parameters

Parameters	A	B	C	ALPHA	BETA	GAMMA
Before optimized	6.5782	6.5782	5.2803	90	90	120
After optimized	7.9184	7.9184	5.1954	89.9995	89.8043	120.9421

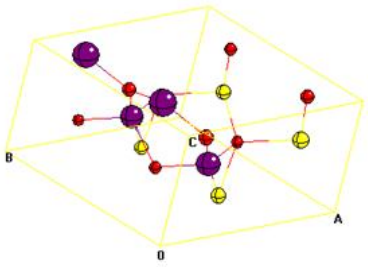

Figure 4.7 $Sr_4Zn_4O_8$ crystal structure.

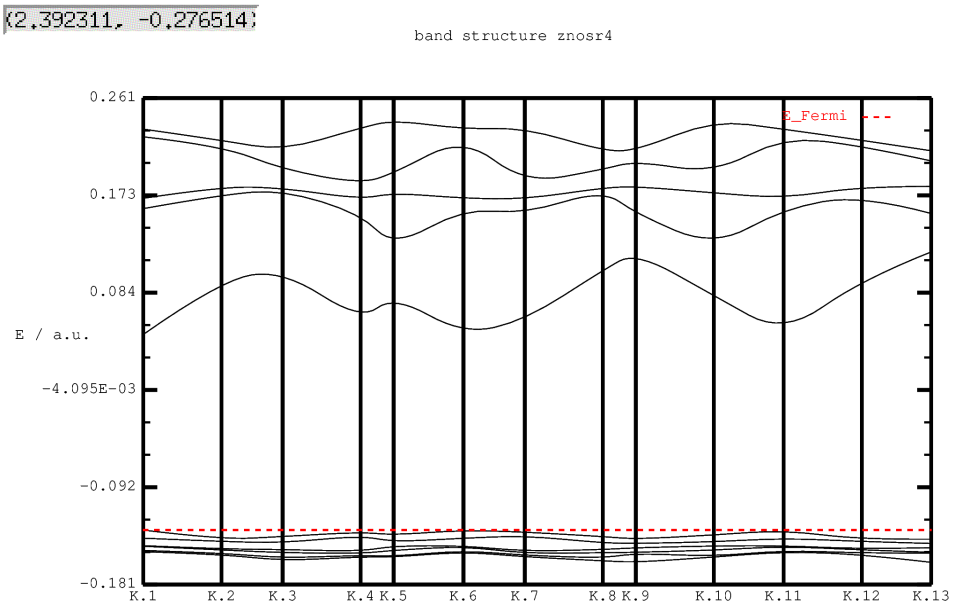

Figure 4.8: Electronic band structure for $Sr_4Zn_4O_8$ .The band gap between the top of the valence band and the bottom of the conduction band ≈4.78 electron Volt.

4.4.5 62.5% doping amount of Sr in ZnO

Table 4 .6: $Sr_5Zn_3O_8$ optimized cell parameters

Parameters	A	B	C	ALPHA	BETA	GAMMA
Before optimized	6.5782	6.5782	5.2803	90	90	120
After optimized	7.2862	7.2862	5.5570	90	90	118.8183

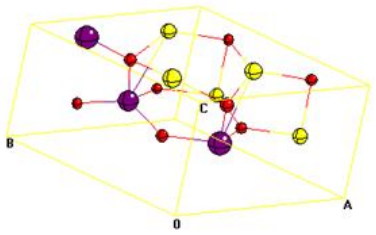

Figure 4.9 $Sr_5Zn_3O_8$ crystal structure.

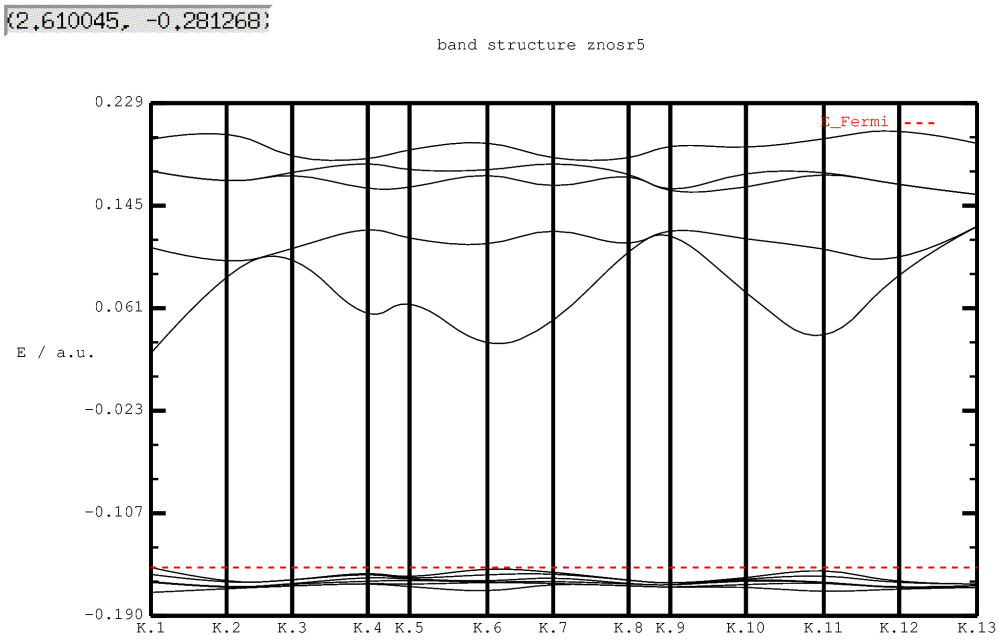

Figure 4.10: Electronic band structure for $Sr_5Zn_3O_8$ .The band gap between the top of the valence band and the bottom of the conduction band ≈4.81 electron Volt.

4.4.6 75% doping amount of Sr in ZnO

Table 4 .7: $Sr_6Zn_2O_8$ optimized cell parameters

Parameters	A	B	C	ALPHA	BETA	GAMMA
Before optimized	6.5782	6.5782	5.2803	90	90	120
After optimized	7.7447	7.7447	5.8753	90	89.3712	119.9689

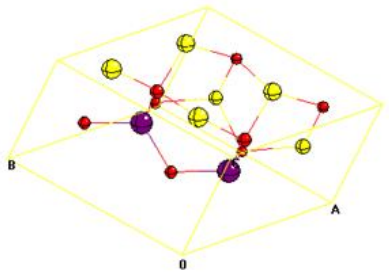

Figure 4.11 $Sr_6Zn_2O_8$ crystal structure.

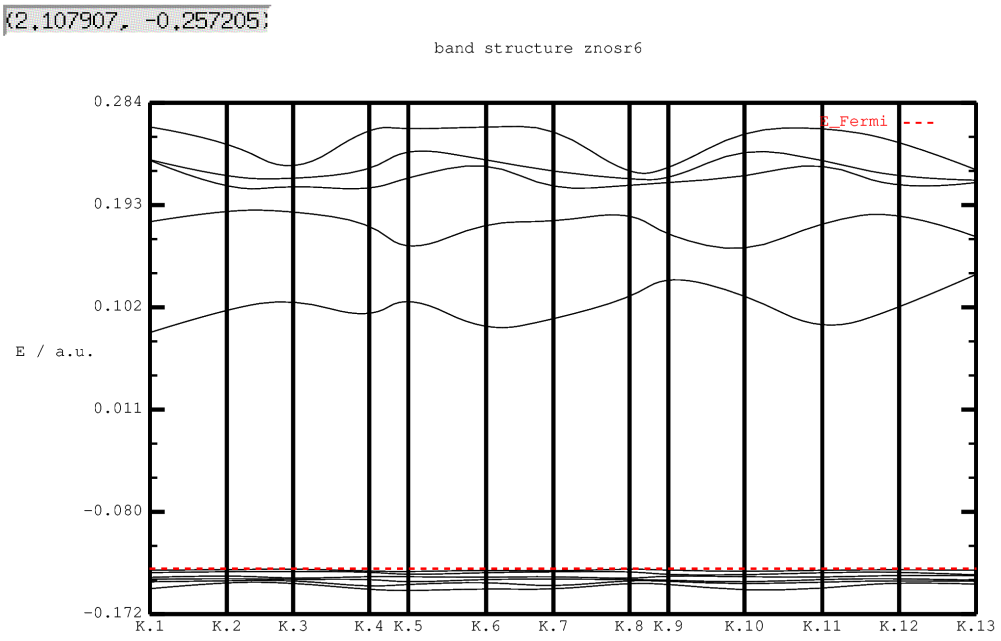

Figure 4.12: Electronic band structure for $Sr_6Zn_2O_8$ .The band gap between the top of the valence band and the bottom of the conduction band ≈5.64 electron Volt.

4.4.7 87.5% doping amount of Sr in ZnO.

Table 4 .8: Sr_7ZnO_8 optimized cell parameters

Parameters	A	B	C	ALPHA	BETA	GAMMA
Before optimized	6.5782	6.5782	5.2803	90	90	120
After optimized	8.4354	8.4354	5.1509	90	90	120

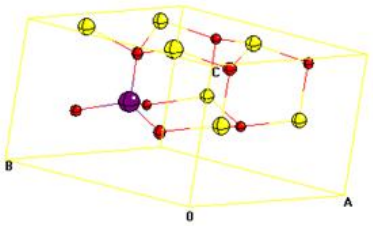

Figure 4.13 Sr_7ZnO_8 crystal structure

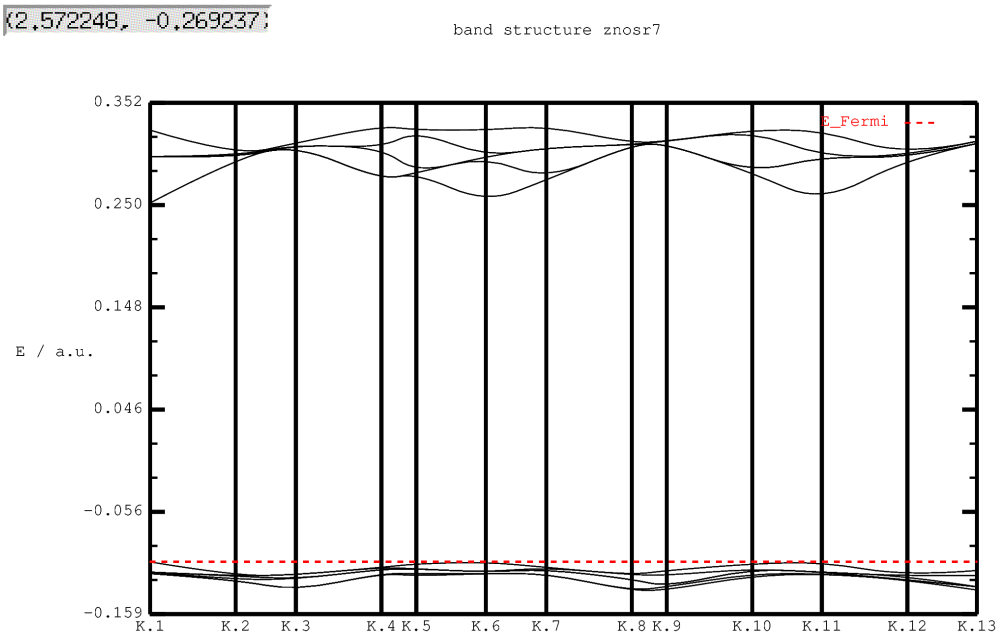

Figure 4.14: Electronic band structure for Sr_7ZnO_8 .The band gap between the top of the valence band and the bottom of the conduction band ≈7.12 electron Volt.

4.4.8 100% doping amount of Sr in ZnO

Table 4 .9: Sr_8O_8 optimized cell parameters

Parameters	A	B	C	ALPHA	BETA	GAMMA
Before optimized	6.5782	6.5782	5.2803	90	90	120
After optimized	7.9119	7.9119	5.8761	90	90	120

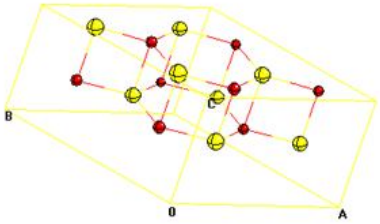

Figure 4.15 Sr_8O_8 crystal structure.

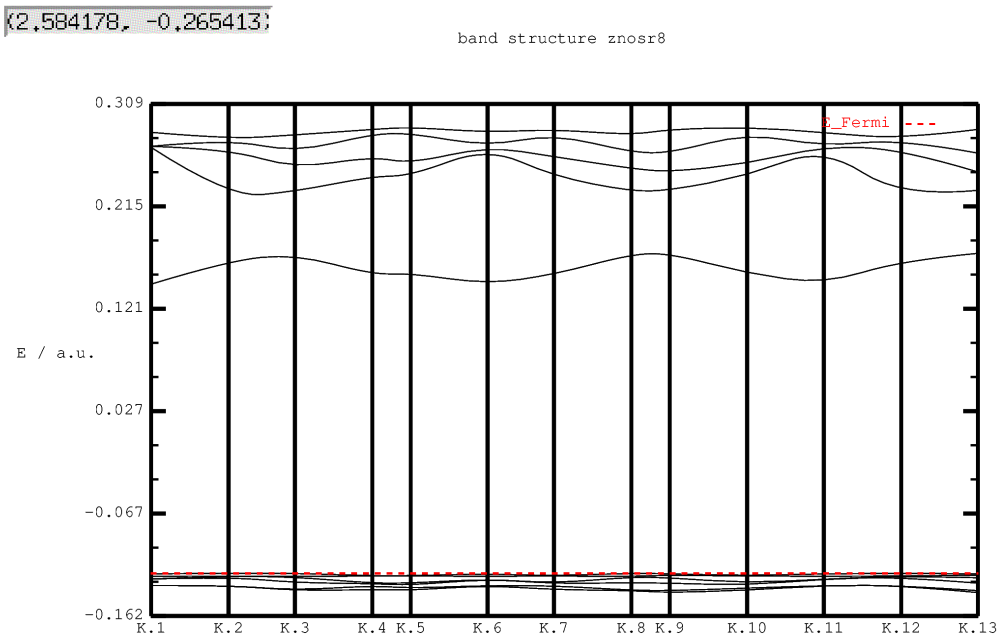

Figure 4.16: Electronic band structure for Sr_8O_8 .The band gap between the top of the valence band and the bottom of the conduction band ≈9.79 electron Volt.

4.5 Conclusion

We used (DFT) with periodic model to discuss electronic structure properties for Sr in ZnO. Once the band gap decrease changes Sr doped ZnO materials have showed as potential energy.

4.6 Recommendations

- We recommended that the study properties electronic ,optical, Solid state, material and semiconductor.
- It can be minimize by the modern technology and nonotechology**.**

References

[1] Bunn C.W (1935) Proc. Phys. Soc. London 47**,** 835.

[2] Moezzi A, et al (2012) Zinc oxide particles: Synthesis, properties and applications Chem. Eng. J. 185**,** 22.

[3] Bates C H, Roy R and White W B (1962) New high-pressure polymorph of zinc oxide Science 137**,** 994.

[4] Nyberg M, etal (1996) Hydrogen dissociation on reconstructed ZnO surfaces J. Phys. Chem. 100, 9063.

[5] P. Hohenberg and W. Kohn. (1964) "Inhomogeneous electron gas". Physical Review B136, 864.

[6] W. Kohn and L. J. Sham, (1965) "Self-Consistent Equations Including Exchange and Correlation Effects", Physical Review A 140, 1133.

[7] Perdew, J.P. and Y. Wang, (1992) "Accurate and simple analytic representation of the electron-gas correlation energy". Physical Review B 45 23.

[8] Carr, etal (1964) "Ground-state Energy of a High-Density Electron Gas". Physical Review 133 (2A), 371.

[9] D. M. Ceperely and B. J. Alder, (1980) "Ground state of the Electron Gas by aStochastic Method". Physical Review letter 45, 566.

[10] D.J. Chadi, M.L. Cohen, (1973) "Special points in the brillouin zone". Physical Review B8, 5747.

[11] J.D. Joannopoulos, M.L. Cohen, (1973) "Electronic charge densities for ZnS in the wurtzite and zincblende structures", Journal of physics, C 6, 1572.

[12] C. Pisani, etal (1988). "Hartree-Fock ab initio treatment of crystalline systems", Lecture Notes in Chemisty, vol. 48, Springer-Verlag, Heidelberg.

[13] C. Pisani, (1996) "Quantum-mechanical ab initio calculation of the properties of crystalline materials", Lecture Notes in chemistry, vol.67, Springer Verlag, Berlin.

[14] [30] Dovesi, et al (2005) "Ab Initio Quantum Simulation in Solid State Chemistry". ChemInform, 36(48), 1.

[15] A. D. Becke, (1993) "Density-Functional Thermochemistry .3. The Role of Exact Exchange", Journal of Chemical Physics 98, 5648.

[16] A. D. becke, (1992) "Density-Functional Thermochemistry .2. The Effect of the Perdew-Wang Generalized-Gradient Correction", Journal of Chemical Physics 97,9173.

[17] A. D. Becke, (1992) "Density-Functional Thermochemistry .1. The Effect of the Exchange-Only Gradient Correction", Journal of Chemical Physics 96,2155.

[18] A. D. Becke, (1997) "Density-Functional Thermochemistry .5. Systematic Optimization of Exchange-Correlation Functionals", Journal of Chemical Physics 107, 8554.

[19] Vosko, et al (1980) " Accurate spin-dependent electron liquid correlation energies for local spin density calculation: a critical analysis". Canadian Journal of Physics 1200.

[20] Doll, et al (2006) "Analutical Hartree-Fock gradients with respect to the cell parameter: systems periodic in one and two dimensions". Theoretical Chemistry Accounts: Theory, Computation, and Modeling (Theoretica Chimica Acta), 115(5), 345.

[21] Broyden, C.G., (1970) "The Convergence of a Class of Double-rank Minimization Algorithms1. General Consideration". IMA Journal of Applied Mathematics 6(1),76.

[22] Fletcher, R., (1970) "A new approach to variable metric algorithms". The computer Journal 13(3), 317.

[23] Goldfarb, D., A Family of Variable-Metric Methods Derived by Variational Means (1970). Mathematics of Computation 24(109), 23.

[24] Lecture Notes on structure of Matter by Mohammad Jellur Rahman, of Physics, BUET, Dhaka-100039. https://www.pubmedcentralCanada.com

[25] Cracknell, A.P.(1969)"Crystals and their Structure", OH. And Hull, D. (1965)"Introduction to Dislocations".

[26] Brando, et al (1999)Microstructural characterization of Materials, Wiley. New York.

[27] Van Bueren, H.G., (1960) Imperfections in Crystals, North Holland, Amsterdan (Wiley-Interscience, New York).

[28] P. Hohenberg and W. Kohn (1964) "Inhomogeneous electron gas". Physical Review B 864, 136.

[29] R. Doves, et al "CRYSTAL06 User's Manual", university of Turin, Torino, Italy, 2006.

[30] A. D. Becke, (1993) "Density-functional thermochemistry. III. The role of exact exchange" Journal of Chemical Physics 98, 5648.

[31] C Lee, et al (1988) "Development of the Colle-Salvetti Correlation-energy formula into a functional of the electron density". Physical Review B 37,785.

[32] J. E. Jaffe and A. C.Hess, (1993) "Hartree-Fock study of phase change in ZnO at high pressure",phys. Rev. B48, 7903.

[33] M.D. Towler, et al (1994)"An ab-initio Hartrre-Fock Study of MnO and NiO ",Phys. Rev. B50, 5041-5054.

[34] M.V.Habas, et al (1998)"B1-B2 Phase Transtion in alkalive-earth Oxides: a caparison of ab-intio Hartree-Fock and density functional calculations", Journal of Physics, Condensed Matter 10, 6897.

[35] Özgür Ü, et al (2005)" A comprehensive review of ZnO materials and devices", J. Appl. Phys. 98 041301.

[36] Özgür Ü, et al (2005)" A comprehensive review of ZnO materials and devices" J. Appl. Phys. 98 041301.